INSTITUTE OF PHYSICS PUBLISHING JOURNAL OF PHYSICS B: ATOMIC, MOLECULAR AND OPTICAL PHYSICS

J. Phys. B: At. Mol. Opt. Phys. **35** (2002) 1025–1034 PII: S0953-4075(02)30192-5

Threshold peaks and structures in vibrational excitation of CH_3I by electron impact

M Allan[1] **and I I Fabrikant**[2]

[1] Department of Chemistry, University of Fribourg, Pérolles, CH-1700 Fribourg, Switzerland
[2] Department of Physics and Astronomy, University of Nebraska, Lincoln, NE 68588-0111, USA

Received 25 October 2001, in final form 31 December 2001
Published 13 February 2002
Online at stacks.iop.org/JPhysB/35/1025

Abstract

Electron energy loss spectra in CH_3I reveal the excitation of the $n\nu_3$ and $\nu_1+n\nu_3$ progressions near threshold, where ν_3 is the C–I stretch and ν_1 the symmetric CH_3 stretch. Relative elastic and vibrationally inelastic cross sections have been measured as a function of electron energy at 135°. They exhibit many sharp structures at the $n\nu_3$, $1\nu_1$ and $2\nu_1$ thresholds. A threshold peak is observed for the excitation of the fundamental $1\nu_3$, but only weak threshold peaks are observed for the higher overtones. The shapes of the cross sections including the sharp structures are well reproduced by a quasiclassical R-matrix resonance theory with non-local potentials. Thermal population of the $1\nu_3$ level permitted the measurement of the superelastic cross section.

1. Introduction

Threshold peaks and various structures are often encountered in vibrational excitation by electron impact near threshold, making this energy region particularly interesting. The threshold peaks, discovered more than 25 years ago by Rohr and Linder (1975, 1976) in hydrogen halides, are large enhancements of cross section in a narrow region above threshold. The structures include narrow cusps, vibrational Feshbach resonances of varying widths, broader oscillatory 'boomerang' structures, and narrow outer well resonances (Cvejanović and Jureta 1989, Čížek *et al* 2001).

Threshold phenomena have been subject to deeper experimental and theoretical studies recently (Allan *et al* 2000, Čížek *et al* 2001). Improved experimental techniques permitted measurements of the cross sections with higher accuracy as far as their shape near threshold is concerned, and at higher resolution. Advances in theory, describing scattering in terms of a non-local complex potential, succeeded spectacularly in describing the shapes of the cross sections and the various narrow structures.

The threshold peaks and structures have been studied primarily in the diatomic hydrogen halides, where the dipole moment plays an important role by binding the electron at large internuclear distances. Threshold peaks have also been reported in both polar and apolar

polyatomic molecules, however—for example H_2O (Seng and Linder 1976) and CO_2 (Kochem *et al* 1985). Sharp threshold structures have recently also been found in the meV resolution studies of electron attachment to clusters (Weber *et al* 1999).

Threshold peaks have been associated with vibrational Feshbach resonances (VFR) and a rule has been proposed in hydrogen halides whereby pronounced threshold peaks are found only below the dissociative electron attachment limit. The absence of threshold peaks has consequently been predicted theoretically by Horáček *et al* (1997) in HI, where the dissociative attachment threshold lies below the zero of the incident electron energy scale. The prediction was confirmed experimentally by Sergenton and Allan (2000). The dissociative attachment threshold is below the zero of the incident electron energy scale in CH_3I as well, adding interest to the question of whether threshold peaks are present or absent in vibrational excitation.

At this point it should be stressed that an ambiguity of terms may arise from the fact that there is a continuous transition between the presence and the absence of threshold peaks. Even in HI the signal onsets are vertical, and the cross sections have large values at threshold and sometimes a weak peak, posing a question of semantics about from which point on the term 'threshold peak' should be used. We apply this term to sharp peaks whose width is substantially smaller than vibrational spacing and whose height is more than perhaps 30% (i.e. approximately the experimental uncertainty) larger than the magnitude of the cross section immediately following the threshold peak.

Current interest further concerns the questions of what molecular or cluster properties are required for the threshold peaks and structures to occur and how widely they are found in polyatomic molecules. In the present work we study the near-threshold phenomena in vibrational excitation of CH_3I both experimentally and theoretically, with the aim of shedding more light on the nature of these phenomena and their relationship to the molecular properties of the target. Narrow structures (cusps and a peak due to a VFR) have already been reported in the meV resolution dissociative electron attachment experiment with CH_3I in Kaiserslautern (Schramm *et al* 1999). An R-matrix calculation in that paper predicted a threshold peak and a structure at the $\nu = 2$ threshold in the excitation of one quantum of the C–I stretch vibration. CH_3I is interesting because of its large polarizability connected with the iodine atom, and because it is chemically related to the hydrogen halides where threshold features have been thoroughly studied.

2. Methods

The measurements were performed using a spectrometer with hemispherical analysers described by Allan (1992, 1995), the resolution and low-energy capability of which have recently been improved (Allan 2001b). The energy of the incident beam was calibrated on the 19.366 eV ^2S resonance in helium and is accurate to within ± 20 meV. The elastic peak appears 14–15 meV (fwhm) wide in the energy loss spectra, indicating an energy spread of about 10 meV in the incident electron beam. The analyser response function was determined on the elastic scattering in helium. The overall response function of the instrument is given by the response function of the analyser and, at low energies, by the fact that the incident electron beam becomes more diffuse. In the present work we do not attempt to separate these two effects as described by Allan (1992), but include both into one effective correction curve. This leads to some error because the cross sections for exciting low-lying vibrational states have thresholds at low energies, where the incident beam is more diffuse and less efficient. We believe that the shapes of the cross sections are reliable to about $\pm 20\%$ at energies higher than about 0.3 eV above threshold, to about $\pm 40\%$ at energies closer to threshold. The sample inlet nozzle had a diameter of 0.25 mm and was kept at $\sim 30\,^{\circ}$C during the measurements.

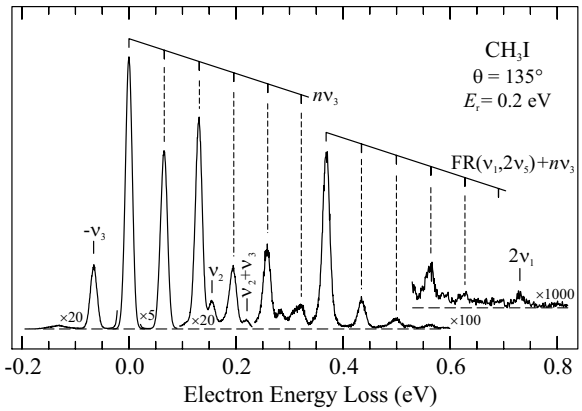

Figure 1. Energy-loss spectrum of CH_3I recorded at a fixed energy of the scattered electrons, $E_r = 0.2$ eV. FR designates the upper member of a dyad resulting from a Fermi resonance between $1\nu_1$ and $2\nu_5$.

The calculations were performed using the quasiclassical R-matrix theory (Fabrikant 1991) which has been successfully applied to dissociative electron attachment to CH_3I as described in detail by Schramm *et al* (1999) and Wilde *et al* (2000). The R-matrix parameters were chosen to reproduce the experimental position and magnitude of the VFR in dissociative attachment cross section below the threshold of excitation of the symmetric stretch ν_3.

3. Results and discussion

The energy loss spectrum shown in figure 1 was recorded by collecting scattered electrons with a fixed residual energy of $E_r = 0.2$ eV and varying the incident electron energy. All the bands were thus recorded 0.2 eV above their respective excitation thresholds. The assignment of the vibrational bands is indicated by vertical bars and grids in figure 1. The energies of these bars, as well as the energies of the bars indicating vibrational thresholds in the remaining figures of this paper, are based on spectroscopic values and anharmonicity constants given by Herzberg and Herzberg (1949) and by Duncan *et al* (1989). The spectroscopic wavenumbers for the $1\nu_3$ and the $2\nu_3$ states are 533.2 and 1059.5 cm^{-1} respectively, and the higher members of the $n\nu_3$ progression are approximated using the anharmonicity constant $x_{33} = -3.44$ cm^{-1}. The wavenumbers of the $1\nu_1$ and the $2\nu_1$ states are 2971.3 and 5891.0 cm^{-1} respectively. The spectrum is seen to be dominated by the progressions $n\nu_3$ and $\nu_1 + n\nu_3$, where ν_3 is the C–I stretch vibration and ν_1 the symmetric CH_3 stretch vibration. There is a Fermi resonance between $1\nu_1$ and the overtone vibration $2\nu_5$, where ν_5 is the degenerate CH_3 deformation. The two coupled states are at 355 and 368 meV and it is predominantly the upper one which is excited in the spectrum of figure 1. The symmetric CH_3 deformation ν_2 is weakly excited. The population of the $1\nu_3$ state relative to that of the vibrational ground state 0^0 is about 8% at our temperature and the superelastic peak is consequently well visible in the figure 1. We do not attempt to correct the cross sections for the thermal population of the $1\nu_3$ state in the present work and the 'elastic' cross section given below thus includes some elastic scattering on CH_3I in the $1\nu_3$ state, the '$0^0 \rightarrow 1\nu_3$ cross section' contains a contribution from the $1\nu_3 \rightarrow 2\nu_3$ transition, etc.

We also recorded a spectrum at the residual energy of 0.05 eV and found it to be very similar to that shown in figure 1. This means that overtone and combination vibrations are

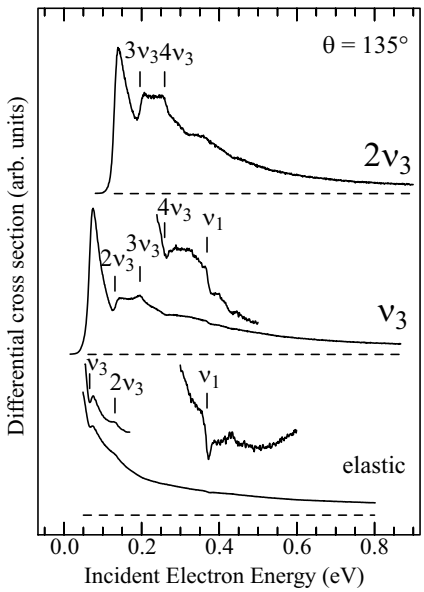

Figure 2. Cross sections for elastic scattering and the excitation of one and two quanta of the C–I stretch vibration ν_3 as indicated on the right. Vibrational thresholds are indicated above the spectra by vertical lines and labels. The visibility of weak structures has been enhanced by showing parts of the spectra vertically expanded and tilted such as to reduce the slope.

significantly excited in CH_3I even at threshold, in contrast to other polyatomic molecules exhibiting threshold peaks like H_2O, CO_2, or *cis*-difluoroethene (Allan *et al* 2002), where excitation of overtone and combination vibrations is very weak.

The elastic cross section and the cross sections for the excitation of one and two quanta of the C–I stretch vibration ν_3 are shown in figure 2. The elastic cross section has structures at the thresholds of the ν_3 and ν_1 vibrations. The inelastic cross sections have threshold peaks and structures at vibrational thresholds. The threshold peaks are not as pronounced as, for example, in HBr. The shape of the ν_3 excitation follows closely the prediction of Schramm *et al* (1999). The shape of the cross section for exciting $2\nu_3$ resembles strongly the $\nu = 0 \rightarrow 2$ cross section in HI (Sergenton and Allan 2000), the cross section for exciting a single quantum of ν_3 has a more substantial threshold peak, in contrast to the $\nu = 0 \rightarrow 1$ cross section in HI, however. This observation can be connected to the barrier to dissociation calculated in CH_3I (Wilde *et al* 2000), which is absent in HI. This barrier leads to a pronounced VFR in dissociative attachment to CH_3I below the $\nu = 1$ threshold (Schramm *et al* 1999). According to the interpretation suggested for hydrogen halides by Teillet-Billy and Gauyacq (1984), the 'tail' of this VFR appears as a sharp peak in the $\nu = 0 \rightarrow 1$ cross section. Our results for CH_3I give perhaps the first example of observation of threshold peak in vibrational excitation *above* the dissociative attachment threshold.

Figure 3 shows the cross sections for the excitation of higher vibrational levels. They all peak at threshold, although the relative heights of the threshold peaks are less than in the $1\nu_3$ cross section. Structures at the $n\nu_3$ thresholds are seen in all the curves, a structure at the $2\nu_1$ threshold appears in the $1\nu_1$ cross section.

Figures 4–6 compare the shapes of the experimental cross sections with the results of the calculation. All the essential features of the experiment are well reproduced. Both the dip at

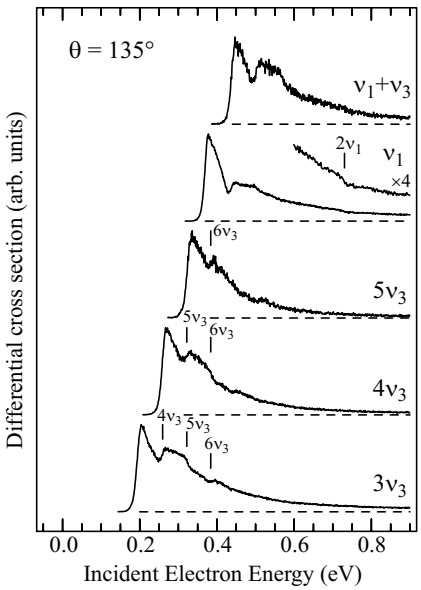

Figure 3. Cross sections for excitation of higher overtones of the C–I stretch vibration ν_3, the fundamental of the ν_1 vibration, and the $\nu_1 + \nu_3$ combination vibration. Vibrational thresholds are indicated above the spectra by vertical lines and labels.

the $1\nu_3$ threshold and the little peak at the $2\nu_3$ threshold are reproduced in the elastic cross section in figure 4. The dip appears at a slightly higher energy in the experiment, but the difference is only about 3 meV, less than the confidence limit of the energy scale calibration, and is not significant. The calculated threshold peak in the $1\nu_3$ channel appears slightly higher than in the experiment in figure 5, but the difference must be considered to be within the error limit of the experiment, because the incident electron energy is only 66 meV at the threshold of this channel, and the quality of the incident electron beam in our instrument starts to deteriorate at such a low energy. The calculation correctly reproduces the structure at the $2\nu_3$ threshold in the $1\nu_3$ channel as a dip, the structure at the $3\nu_3$ threshold as a peak. The structures, particularly at higher energies, appear more pronounced in the experiment than in the theory. The shape of the structure in the $2\nu_3$ channel is also reproduced in detail. The structure at the $3\nu_3$ threshold is an upward step, the structure at the $4\nu_3$ threshold is a narrow peak followed by a downward step, the structure at the $5\nu_3$ threshold is a dip. The dip is, again, more pronounced in the experiment than in the theory. The structures in the higher channels shown in figure 6 take the form of alternating upward and downward steps at the vibrational thresholds, very similar to those observed for example in the higher channels of HCl (Schafer and Allan 1991). A difference between theory and experiment is found for the higher final channels: the experimental cross sections fall off faster with increasing energy than predicted by theory at higher incident electron energies. This difference could presumably be reduced by an improved choice of the R-matrix parameters, especially the R-matrix surface amplitude. Indeed, whereas our choice of the resonant potential energy surface is in accord with the results of *ab initio* calculations (Wilde *et al* 2000), the surface amplitude is an empirical parameter in our calculation which was fitted to reproduce the shape of experimentally observed VFR at 66 meV. The shape of VFR is determined by non-adiabatic coupling between vibrational states, and is not very sensitive to the surface amplitude. However, at higher energies inelastic

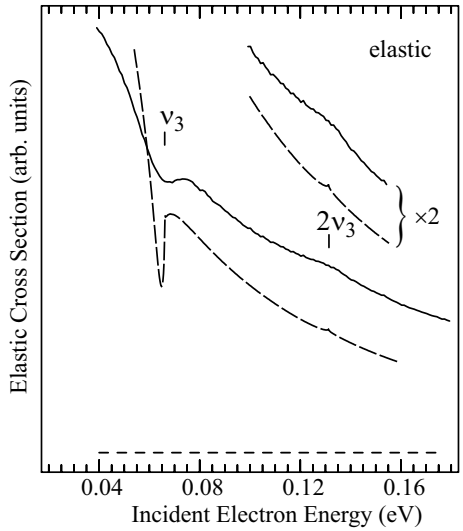

Figure 4. Comparison of the experimental vibrationally elastic cross section (full curve) with theory (broken curve). The vertical scales were chosen arbitrarily for a convenient comparison of shapes. The expanded curves are vertically offset.

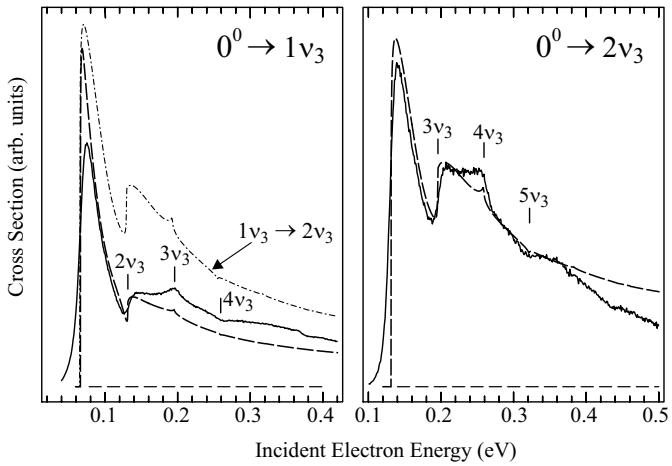

Figure 5. Comparison of the experimental cross sections (full curves) with theory (broken curves) for the transitions indicated in the upper right corners. The vertical scales were chosen arbitrarily for a convenient comparison of shapes. The calculated cross section for the $1\nu_3 \rightarrow 2\nu_3$ cross section is shown by a thinner dash-dotted curve in the left panel, on the same vertical scale as the calculated $0^0 \rightarrow 1\nu_3$ cross section.

cross sections are controlled by the broad shape resonance whose width is directly determined by the R-matrix surface amplitude.

Another drawback of the theory is the neglect of coupling of the ν_3 mode with other modes. This approximation might overestimate the flux in the ν_3 channel at higher energies making the cross sections seem to decay too slowly.

The appreciable thermal population of the $1\nu_3$ vibrational state permitted us to measure the $1\nu_3 \rightarrow 0^0$ superelastic cross section, shown in figure 7. From the theoretical point of view

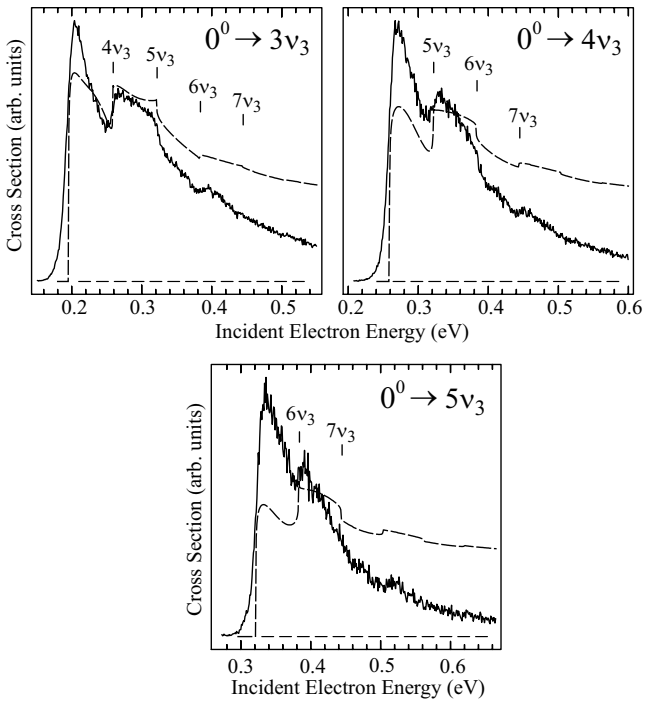

Figure 6. Comparison of the experimental cross sections (full curves) with theory (broken curves) for higher final states. See caption of figure 5.

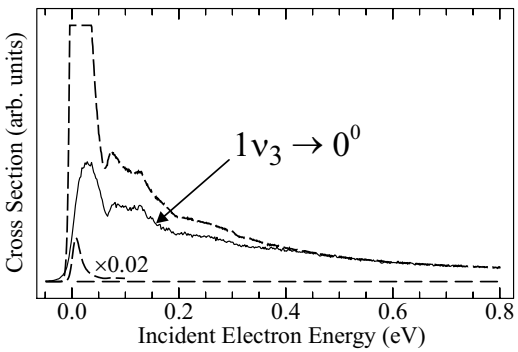

Figure 7. The superelastic cross section (full curve), compared to the cross section obtained from the $0^0 \rightarrow 1\nu_3$ inelastic cross section by applying the detailed balance relation (broken curves).

the superelastic cross section is trivial, all our calculated cross sections automatically satisfy the detailed balance. The comparison of the measured superelastic and inelastic cross sections is included here because it provides a useful test of the quality of the electron beam at low energies and the response correction procedure.

Figure 7 compares the measured superelastic cross section with the inelastic cross section transformed by the detailed balance relation. Both curves were put onto the same relative vertical scale assuming that the population of the vibrational ground state 0^0 is 12.5 times larger than the population of the $1\nu_3$ state. The transformation shifts the inelastic cross section

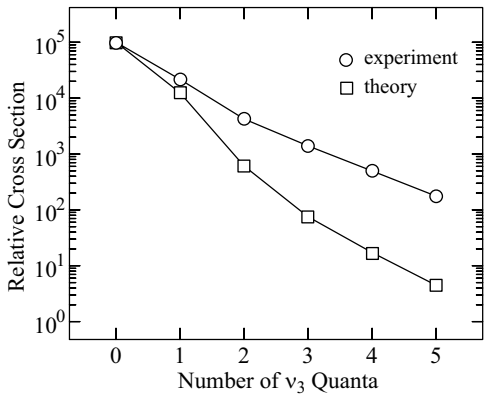

Figure 8. Comparison of the relative magnitudes of the experimental differential cross sections and the theoretical integral cross sections. The vibrationally inelastic cross sections are taken at the first peak above threshold, the elastic cross section is taken at the energy of the peak of the $1\nu_3$ cross sections, which is 68 meV in the theory and 75 meV in the experiment (because of finite resolution). The two data sets are arbitrarily normalized at the leftmost point.

(figure 2) to the left by 66 meV and multiplies it by the factor $(E+\Delta E)/E$, that is, it dramatically expands it vertically at low energies. (We convoluted the factor with a simulated instrumental resolution to take into account the finite energy spread in the incident electron beam and to avoid the pole in the converting factor at $E = 0$.)

The two curves agree satisfactorily in shape down to an energy of about 50 meV. The measured superelastic cross section is dramatically too low below 50 meV, however, because of the rapidly deteriorating quality of the incident electron beam. Note that the measurement of the superelastic cross section requires an incident energy $E_i = 0$ at threshold, which is very hard to realize, whereas the measurement of the inelastic cross section at threshold requires an incident energy of 66 meV, which can be achieved with the present instrument. Figure 7 thus confirms that the response correction procedure is valid within the confidence limits given in the experimental section and that the incident electron beam could be sustained reasonably well down to 50 meV. A further improvement of the instrumental response at low energies is desirable, however.

The measured superelastic cross section is found to be lower than the curve derived from the detailed balance even in the range up to 0.4 eV. This is due in part to errors in correcting for the instrumental response function, but also to the fact that the measured cross sections are 'contaminated' by contributions from thermally excited vibrational levels. The measured $0^0 \rightarrow 1\nu_3$ cross section is superimposed on the $1\nu_3 \rightarrow 2\nu_3$ cross sections and, similarly, the superelastic $1\nu_3 \rightarrow 0^0$ and the $2\nu_3 \rightarrow 1\nu_3$ transitions overlap. The effect of the overlap is increased by the larger magnitude of the cross sections for transitions from excited vibrational levels—our calculation shown in figure 5 indicates, as an example, that the cross section for the $1\nu_3 \rightarrow 2\nu_3$ transition is about two times larger than that for the $0^0 \rightarrow 1\nu_3$ transition (except in the first 50 meV above threshold, where the $0^0 \rightarrow 1\nu_3$ cross section is enhanced by a threshold peak).

Although absolute cross sections have not been measured in the course of this work, it is of interest to know how the ratios of the calculated and measured cross sections compare. The experimental relative cross sections at energies 0.2 eV above threshold have been determined from the relative peak heights in the spectrum of figure 1. The relative cross sections at other energies have then been derived using the excitation functions in figures 2 and 3. The relative

magnitudes of the inelastic cross sections, always at the first peak above threshold, and of the elastic cross sections, at the energies of the peaks of the $1\nu_3$ cross sections, are compared in figure 8. The theoretical elastic and $1\nu_3$ cross sections have already been given by Schramm *et al* (1999). The comparison is only qualitative because integral theoretical cross sections are compared with differential experimental cross sections and because of the relatively large error bar of the experiment very close to threshold. The figure shows that the theoretical cross sections drop faster with increasing vibrational quantum than the experimental ones. We ascribe the difference, apart from the experimental uncertainties, to the same factors as those invoked above to rationalize the differences of cross sectional shapes for the higher vibrational quanta, that is to the choice of the model parameters and the neglect of vibrational channels other than $n\nu_3$.

4. Conclusions

Within the semantic convention discussed in the introduction a threshold peak does exist in the $0^0 \rightarrow 1\nu_3$ cross section of CH_3I, but does not in the $\nu = 0 \rightarrow 1$ cross section of HI. This can be rationalized by the proposition of Schramm *et al* (1999) and Wilde *et al* (2000) that a barrier towards dissociation is present on the potential surface of CH_3I^- (but not of HI^-). The shallow well behind the barrier supports a VFR for the $1\nu_3$ vibrational level, but not for the higher quanta. On the other hand the shapes of the cross sections for the excitation of higher quanta of the C–I stretch in CH_3I are very similar to the corresponding cross sections of HI, the chemical similarity between the two molecules results in similar scattering properties.

The validity of the present theoretical model is borne out by the excellent agreement of the shapes of the threshold peaks and various structures with experiment. The two differences between the calculated and the observed cross sections, the slower fall-off of the calculated cross section profiles with electron energy for the higher final channels and the faster drop of the peak cross sections with increasing number of ν_3 quanta, may indicate the need for a better choice of R-matrix parameters and for inclusion of coupling between the ν_3 mode and other vibrational modes.

The sharp structures in the present cross sections appear to be closely related to the polarizability of the iodine atom, because the chemically related, but less polarizable, CH_3F has threshold peaks, but without structures (Allan 2001a). The situation resembles the CO_2/CS_2 pair, where threshold peaks have no structures in CO_2 (Kochem *et al* 1985, Allan 2001b), but sharp structures in the more polarizable CS_2 (Allan 2001c). A further consequence of the higher polarizability appears to be that overtone vibrations (progressions in ν_3) are significantly excited at threshold in CH_3I, in contrast to many less polarizable polyatomic molecules with threshold peaks.

Future work should include absolute measurements over a wider range of scattering angles, which would reveal possible contributions of higher partial waves and enable comparison of absolute cross sections. A fully *ab initio* determination of the resonance parameters and the inclusion of more vibrational modes in the calculation would be desirable.

Acknowledgments

This research is part of the projects 2000-061543.00 of the Swiss National Science Foundation and PHY-0098459 of the US National Science Foundation. We thank Aschwin Gopalan (Kaiserslautern) for assistance during the measurements.

References

Allan M 1992 *J. Phys. B: At. Mol. Opt. Phys.* **25** 1559
Allan M 1995 *J. Phys. B: At. Mol. Opt. Phys.* **28** 5163
Allan M 2001a *EMS 2001 Symp. (University of Nebraska)* p 67 (Abstracts)
Allan M 2001b *Phys. Rev. Lett.* **87** 033201
Allan M 2001c *22nd Int. Conf. on Photonic, Electronic and Atomic Collisions (Santa Fe, USA)* p 275 (Abstracts)
Allan M, Čížek M, Horáček J and Domcke W 2000 *J. Phys. B: At. Mol. Opt. Phys.* **33** L209
Allan M, Craig N C and McCarty L V 2002 *J. Phys. B: At. Mol. Opt. Phys.* at press
Čížek M, Horáček J, Allan M, Sergenton A-C, Popović D B, Domcke W, Leininger T and Gadea F X 2001 *Phys. Rev.* A **63** 062710
Cvejanović S and Jureta J 1989 *3rd Eur. Conf. on Atomic and Molecular Physics (Bordeaux)* p 638 (Abstracts)
Duncan J L, Ferguson A M and Mathews S 1989 *J. Chem. Phys.* **91** 783
Fabrikant I I 1991 *Phys. Rev.* A **43** 3478
Herzberg G and Herzberg L 1949 *Can. J. Res.* B **27** 332
Horáček J, Domcke W and Nakamura H 1997 *Z. Phys.* D **42** 181
Kochem K H, Sohn W, Nebel N, Jung K and Ehrhardt H 1985 *J. Phys. B: At. Mol. Phys.* **18** 4455
Rohr K and Linder F 1975 *J. Phys. B: At. Mol. Phys.* **8** L200
Rohr K and Linder F 1976 *J. Phys. B: At. Mol. Phys.* **9** 2521
Schafer O and Allan M 1991 *J. Phys. B: At. Mol. Opt. Phys.* **24** 3069
Schramm A, Fabrikant I I, Weber J M, Leber E, Ruf M W and Hotop H 1999 *J. Phys. B: At. Mol. Opt. Phys.* **32** 2153
Seng G and Linder F 1976 *J. Phys. B: At. Mol. Phys.* **9** 2539
Sergenton A-C and Allan M 2000 *Chem. Phys. Lett.* **319** 179
Teillet-Billy D and Gauyacq J P 1984 *J. Phys. B: At. Mol. Phys.* **17** 4041
Weber J M, Leber E, Ruf M-W and Hotop H 1999 *Phys. Rev. Lett.* **82** 516
Wilde R S, Gallup G A and Fabrikant I I 2000 *J. Phys. B: At. Mol. Opt. Phys.* **33** 5479